View Article Online / Journal Homepage / Table of Contents for this issue

The annular tautomerism of the curcuminoid NH-pyrazoles†

Pilar Cornago,*[a] Pilar Cabildo,[a] Rosa M. Claramunt,[a] Latifa Bouissane,[a] Elena Pinilla,[b] M. Rosario Torres[b] and José Elguero[c]

Received (in Montpellier, France) 16th July 2008, Accepted 10th October 2008
First published as an Advance Article on the web 2nd December 2008
DOI: 10.1039/b812018h

Published on 02 December 2008 on http://pubs.rsc.org | doi:10.1039/B812018H
Downloaded on 02 January 2013

The structures of four NH-pyrazoles, (*E*)-3,5-bis[β-(4-hydroxy-3-methoxyphenyl)-ethenyl]-1*H*-pyrazole (**3**), (*E*)-3(5)-[β-(4-hydroxy-3-methoxyphenyl)-ethenyl]-5(3)-methyl-1*H*-pyrazole (**4**), (*E*)-3(5)-[β-(4-hydroxy-3-methoxyphenyl)-ethenyl]-4,5(3)-dimethyl-1*H*-pyrazole (**5**) and (*E*)-3(5)-[β-(3,4-dimethoxyphenyl)-ethenyl]-4-methyl-5(3)-phenyl-1*H*-pyrazole (**8**), have been determined by X-ray crystallography. Compounds that have a phenol residue crystallize forming sheets that are stabilized by a complex pattern of hydrogen bonds between a unique tautomer (**4**), or by a 2 : 1 mixture of both tautomers (**5**) (these tautomers being identical in the case of **3**). Pyrazole **8**, which lacks OH groups, crystallizes in cyclic dimers that are stabilized by N–H···N hydrogen bonds. The tautomerism in solution and in the solid state was determined by ^{13}C and ^{15}N CPMAS NMR spectroscopy. For compounds **4**, **5** and **8**, the solid state results agree with those observed by crystallography; the most abundant tautomer in solution coincides with the tautomer present in the solid state (**4** and **8**) or with the most abundant tautomer in the crystal (**5**).

Introduction

Turmeric is a spice derived from the rhizomes of *Curcuma longa*, which is a member of the ginger family.[1] The bright yellow color of turmeric comes mainly from polyphenolic pigments known as curcuminoids. Curcumin (**1**) (Scheme 1) is the principal curcuminoid found in turmeric, and is generally considered to be its most active constituent. In addition to its use as a spice and a pigment, turmeric has been used in India for medicinal purposes for centuries. More recently, evidence that **1** may have anti-inflammatory and anti-cancer activities has renewed scientific interest in its potential to prevent and treat disease. **1** is also an effective scavenger of reactive oxygen and nitrogen species *in vitro*. In addition to its direct antioxidant activity, **1** has been found to inhibit PLA2, COX-2 and 5-LOX activity in cultured cells. It has also been found to inhibit NF-κB-dependent gene transcription, and to inhibit the induction of COX-2 and iNOS in cell culture and animal studies.[2] **1** has been found to induce cell cycle arrest and apoptosis in a variety of cancer cell lines grown in cultures. The ability of **1** to induce apoptosis in cultured cancer cells has generated scientific interest in its potential to prevent some types of cancer. Oral administration of **1** has been found to inhibit the development of chemically-induced cancer in animal models of oral, stomach, liver and colon cancer.

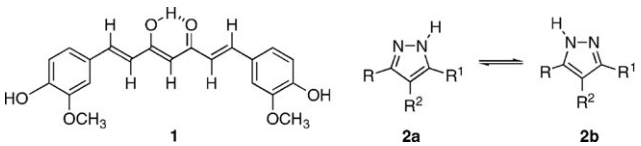

Scheme 1 The structure of curcumin (**1**) and the tautomerism of pyrazoles **2**.

We have devoted a series of papers to the annular tautomerism of NH-pyrazoles **2** (**2a** *vs.* **2b**),[3,4] and decided to study those derived from **1** and related β-diketones.

Pyrazole **3**, which is derived from **1**, has been prepared many times since 1991.[5–11] It has been described as a pale yellow solid that melts at 211–214[5] or 215[7] °C.

The activity of the curcuminoid pyrazoles covers domains such as anti-inflammatory (5-lipooxygenase and cyclooxygenase inhibitors)[5,8] and anti-tumoral (anti-angiogenic)[6–8] agents, and drugs for the treatment of Alzheimer's disease (AD; potent γ-secretase inhibitors, potent ligands for fibrillar Ab42 aggregates, tau aggregation inhibitors and depolymerizing agents for tau aggregates).[10,11] Particularly promising for treating reduced cognitive functions is 4,4′-[(1-phenyl-1*H*-pyrazole-3,5-diyl)di-(1*E*)-2,1-ethenediyl]bis(2-methoxyphenol) (CNB-001), the product obtained by reacting **1** with phenylhydrazine.[12] In the last of these applications, curcumin-derived pyrazoles were synthesized in order to minimize the metal chelation properties of **1**. The reduced rotational freedom and the absence of stereoisomers were anticipated to enhance the inhibition of γ-secretase. Accordingly, the replacement of the 1,3-dicarbonyl moiety by isosteric heterocycles, such as pyrazoles, turned these compounds into very interesting candidates for AD research.

[a] *Departamento de Química Orgánica y Bio-Orgánica, Facultad de Ciencias, UNED, Senda del Rey 9, E-28040 Madrid, Spain. E-mail: mcornago@ccia.uned.es; Fax: +34 913988372; Tel: +34 913987323*
[b] *Departamento de Química Inorgánica I, Facultad de Ciencias Químicas, Universidad Complutense de Madrid (UCM), 28040 Madrid, Spain*
[c] *Instituto de Química Médica, CSIC, Juan de la Cierva 3, E-28006 Madrid, Spain*

† CCDC reference numbers 690489–690492. For crystallographic data in CIF or other electronic format see DOI: 10.1039/b812018h

Published on 02 December 2008 on http://pubs.rsc.org | doi:10.1039/B812018H
Downloaded on 02 January 2013

The aim of this paper is to determine and discuss the structure, tautomerism and possible proton transfer in the solid state (SSPT) of six NH-pyrazoles by using a combination of X-ray crystallography and $^{13}C/^{15}N$ NMR spectroscopy.

The nomenclature used in the text and in the experimental is not in accordance with IUPAC rules. For all of the compounds with phenolic hydroxyl groups, **3**–**6**, the phenol system has the highest priority; however, using IUPAC nomenclature here would be at the expense of comparability and clearness. For instance, compound **4** would be 2-methoxy-4-[(*E*)-2-(5-methyl-1*H*-pyrazol-3-yl)vinyl]phenol under IUPAC rules, rather than (*E*)-3(5)-[β-(4-hydroxy-3-methoxyphenyl)ethenyl]-5(3)-methyl-1*H*-pyrazole. In order to prioritize comparability over correct nomenclature, we have named all of the compounds as pyrazole derivatives.

Results and discussion

Synthesis

All of the compounds discussed in this work (Scheme 2) are reported in the experimental section. They were prepared by the reaction of hydrazine with the corresponding β-diketone, the most common method of synthesizing pyrazoles,[13] which in the case of **3** was **1**.[14]

X-Ray structure determination

The structures of pyrazoles **3** (derived from **1**), **4**, **5** and **8** have been determined by X-ray crystallography.

Concerning tautomerism, in the case of **3**, tautomers **3a** and **3b** are identical. In the case of **4**, the only tautomer present is 3-(3-methoxy)-4-hydroxy-styryl-5-methyl-1*H*-pyrazole (**4a**). In the case of **5**, there is a 2 : 1 mixture of 3-(3-methoxy)-4-hydroxy-styryl-4,5-dimethyl-1*H*-pyrazole (**5a**) and 3,4-dimethyl-5-(3-methoxy)-4-hydroxy-styryl-1*H*-pyrazole (**5b**). In the case of **8**, the only observed tautomer is 3-phenyl-4-methyl-5-(3-methoxy)-4-hydroxy-styryl-1*H*-pyrazole (**8b**). The main data are collected in Table 1 and Table 2. A characteristic feature of the geometry of NH-pyrazoles is that the angle centered at N1 (the atom bearing the NH proton) is always larger than that centered at N2, about 112 and 104°, respectively.[15]

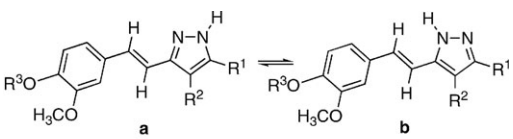

	R^1	R^2	R^3
3		H	H
4	CH_3	H	H
5	CH_3	CH_3	H
6	C_6H_5	H	H
7	C_6H_5	H	CH_3
8	C_6H_5	CH_3	CH_3

3a = 3b

Scheme 2 The structures of the NH-pyrazoles.

Table 1 The bond lengths (Å) and angles (°) for compounds **3**, **4**, **8** and the three crystallographically-independent molecules of **5**

	3	**4**	**5**(1)	**5**(2)	**5**(3)	**8**
N1–N2	1.354(3)	1.365(3)	1.349(4)	1.352(4)	1.359(3)	1.351(3)
N2–C3	1.347(4)	1.339(3)	1.341(5)	1.348(5)	1.349(5)	1.339(4)
C3–C4	1.399(4)	1.398(4)	1.388(6)	1.410(5)	1.401(6)	1.415(4)
C4–C5	1.373(4)	1.369(3)	1.381(6)	1.366(5)	1.374(6)	1.379(4)
C5–N1	1.353(4)	1.340(3)	1.332(6)	1.346(5)	1.331(5)	1.360(4)
C3–C6	1.445(4)	1.453(3)	—	1.463(5)	1.450(6)	1.377(3)
C5–C6	—	—	1.446(7)	—	—	1.444(4)
C6–C7	1.327(4)	1.325(3)	1.309(1)	1.310(6)	1.304(4)	1.333(4)
C7–C8	1.467(4)	1.472(3)	1.460(1)	1.457(5)	1.475(6)	1.460(4)
C3–C15	—	—	1.484(6)	—	—	—
C5–C15	1.450(4)	1.484(2)	—	1.490(5)	1.509(6)	—
C15–C16	1.322(4)	—	—	—	—	—
C16–C17	1.463(4)	—	—	—	—	—
C10–O2	1.376(4)	1.367(3)	1.359(6)	1.367(4)	1.372(5)	1.372(3)
O2–C14	1.433(4)	1.419(3)	1.424(6)	1.430(5)	1.442(5)	1.416(4)
C11–O1	1.368(4)	1.369(3)	1.372(5)	1.361(5)	1.363(5)	1.371(3)
C15–O1	—	—	—	—	—	1.418(4)
C19–O4	1.366(4)	—	—	—	—	—
O4–C23	1.416(4)	—	—	—	—	—
C20–O3	1.382(4)	—	—	—	—	—
N2–N1–C5	112.2(3)	112.7(2)	112.2(4)	111.8(3)	111.6(3)	112.4(2)
N1–N2–C3	105.3(2)	104.4(2)	104.4(3)	105.2(3)	104.7(3)	105.3(2)

Crystals of sufficient quality for X-ray diffraction analysis were obtained for compounds **3** (1 : 1 H_2O/EtOH), **4** (1 : 1 : 1 CH_2Cl_2/hexane/EtOH), **5** (1 : 1 : 1 CH_2Cl_2/hexane/EtOH) and **8** (1 : 1 : 1 CH_2Cl_2/hexane/EtOH) from their respective solvent mixtures. Table 1 shows selected bond lengths and angles for each of these compounds, and Table 2 shows the distances and angles of the intermolecular hydrogen bonds.

One crystallographically-independent molecule was identified in the structural determination of **3**, where the pyrazole and phenyl rings were co-planar, with bond distances and angles within normal ranges (Fig. 1). The intermolecular hydrogen bonds led to layers parallel to (1 0 1), as shown in Fig. 2.

Table 2 The bond lengths (Å) and angles (°) for the hydrogen bonds in compounds **3**, **4**, **5** and **8**

Compound	D–H···A	$d_{D–H}$	$d_{H···A}$	$d_{D···A}$	∠$_{D–H···A}$
3	O3–H3···O4	1.10	1.98	2.647(4)	115.1
	N1–H1B···O3^a	1.06	1.93	2.864(4)	144.7
	O1–H1A···N2^b	1.17	1.79	2.811(4)	142.7
	O3–H3···O1^c	1.10	2.26	2.825(4)	108.7
4	O1–H1A···N2^d	0.99	1.86	2.832(3)	167.5
	N1–H1B···O2^e	1.07	2.17	2.962(3)	128.6
5	O13–H113···N21	1.16	1.81	2.782(5)	137.3
	N12–H12···N23	1.10	1.82	2.914(5)	175.6
	O11–H111···O13^f	0.92	2.03	2.813(4)	141.3
	O12–H112···N22^g	1.14	1.57	2.673(4)	159.4
	N11–H11···O11^g	1.08	2.01	2.951(5)	144.3
	N13–H13···O12^i	1.02	1.93	2.853(4)	148.6
8	N1–H1···N2^j	0.90(4)	2.07(4)	2.872(3)	147(4)

Symmetry transformations used to generate equivalent atoms: ^{a} $-x+2, y-\frac{1}{2}, -z+\frac{1}{2}$. ^{b} $-x+1, y+\frac{1}{2}, z+\frac{3}{2}$. ^{c} $x+1, y, z-1$. ^{d} $-x+1, -y+2, -z+1$. ^{e} $x, -y+\frac{3}{2}, z-\frac{1}{2}$. ^{f} $-x+4, y-\frac{1}{2}, -z+\frac{3}{2}$. ^{g} $-x+1, y-\frac{1}{2}, -z+\frac{1}{2}$. ^{h} $-x+4, y+\frac{1}{2}, -z+\frac{3}{2}$. ^{i} $-x+1, y+\frac{1}{2}, -z+\frac{1}{2}$. ^{j} $-x+2, -y, -z+1$.

 This journal is © The Royal Society of Chemistry and the Centre National de la Recherche Scientifique 2009

Published on 02 December 2008 on http://pubs.rsc.org | doi:10.1039/B812018H
Downloaded on 02 January 2013

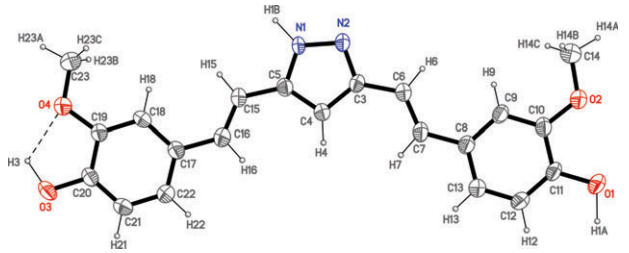

Fig. 1 The X-ray molecular structure of compound **3** (ORTEP plot, 35% probability for the ellipsoids).

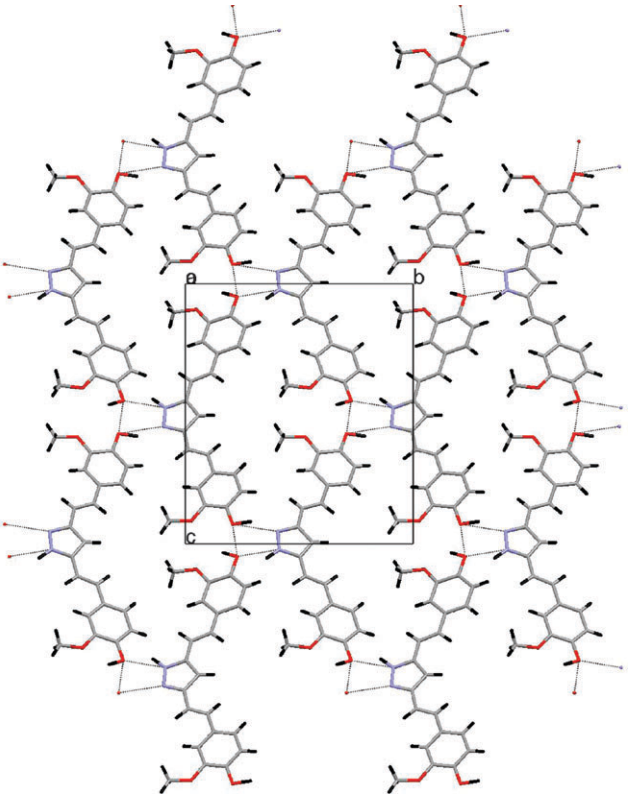

Fig. 2 The view along the a axis of **3**, showing the formation of layers due the intermolecular hydrogen bonds.

Fig. 3 shows an ORTEP representation of the asymmetric unit of compound **4**, a non-planar molecule with a dihedral angle of 19.0(1)° between the pyrazole and phenyl rings. Dimers (O1–H1A–N2) linked by hydrogen bonds

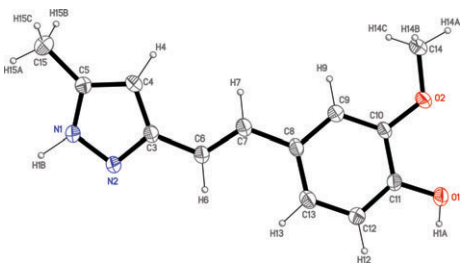

Fig. 3 The X-ray molecular structure of compound **4** (ORTEP plot, 35% probability for the ellipsoids).

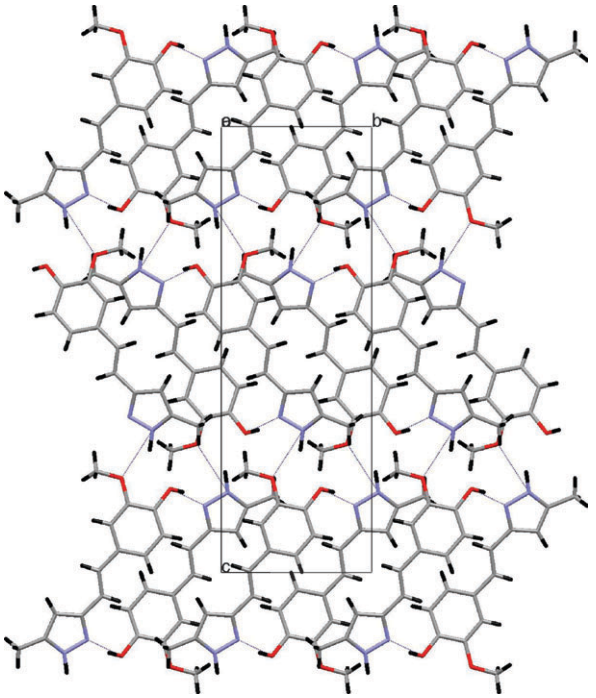

Fig. 4 The view along the b axis of **4**, showing the formation of layers due the intermolecular hydrogen bonds.

(N1–H1B–O2) led to layers parallel to (1 0 0), as shown in Fig. 4.

The asymmetric unit of compound **5** is presented in Fig. 5. The crystal consists of three crystallographically-independent, almost planar molecules, held together by hydrogen bonds that form a trimer, which, through additional hydrogen bonding, forms layers parallel to (–1 0 3), as shown in Fig. 6.

Fig. 7 shows the non-planar molecule of compound **8**, with a dihedral angle of 15.7(1)° between the pyrazole and the phenyl ring at the 3-position, and 36.5(1)° between the pyrazole and the phenyl ring of the styryl group at the 5-position. Molecules of **8** are centrosymmetrically linked by hydrogen bonds (Table 2), giving rise to dimers, and these species are within van der Waals distances (Fig. 8).

The cyclic N–H···N hydrogen-bonded motifs (cyclamers) of NH-pyrazoles have been studied on several occasions.[4d,16,17] These motifs are characteristic of NH-pyrazoles lacking substituents that bear hydrogen bonding functional groups, such as –OH or –CO_2H. These groups, as well as solvent molecules like H_2O and ROH, participate in the hydrogen bonding network that determines the secondary structure of the crystals, destroying the $(N–H···N)_n$ hydrogen bonds.[18–20] In three of the compounds described in the present paper, those bearing phenol groups (**3**, **4** and **5**) form several hydrogen bonds involving the OH group: **3** (O–H···N, N–H···O, O–H···O), **4** (O–H···N, N–H···O) and **5** (O–H···N, N–H···O, O–H···O, N–H···N; present as two molecules of tautomer **5a** and one molecule of tautomer **5b**). In the case of **8**, which lacks phenol groups, the compound crystallizes as a dimer. This kind of cyclamer is characteristic of NH-pyrazoles that are substituted with phenyl groups at the 3- and 5-positions,[16] to which compound **8** is clearly related.

Published on 02 December 2008 on http://pubs.rsc.org | doi:10.1039/B812018H
Downloaded on 02 January 2013

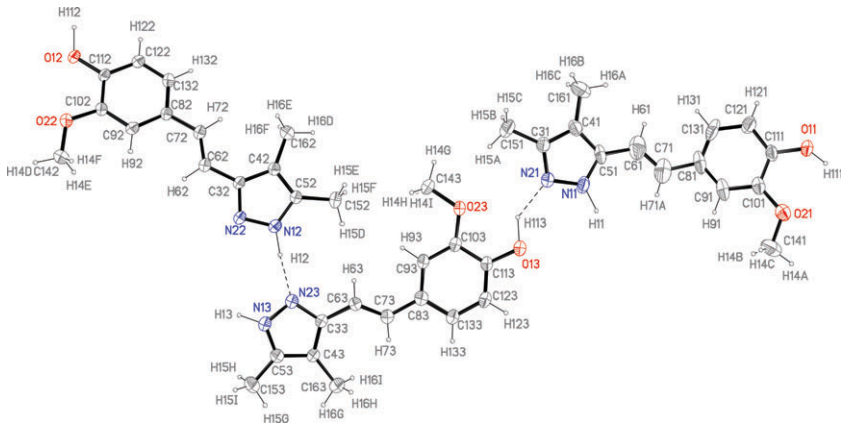

Fig. 5 The X-ray molecular structure of compound **5** (ORTEP plot, 40% probability for the ellipsoids).

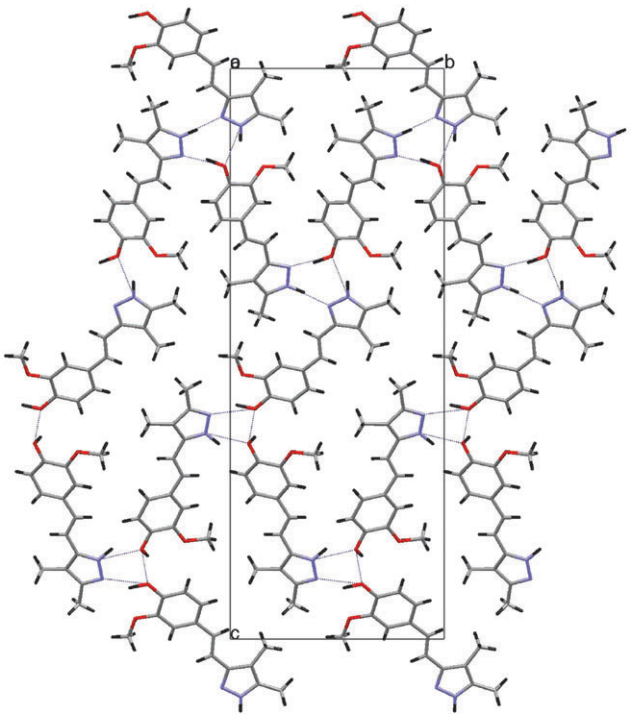

Fig. 6 The view along the a axis of **5**, showing the formation of layers due the intermolecular hydrogen bonds.

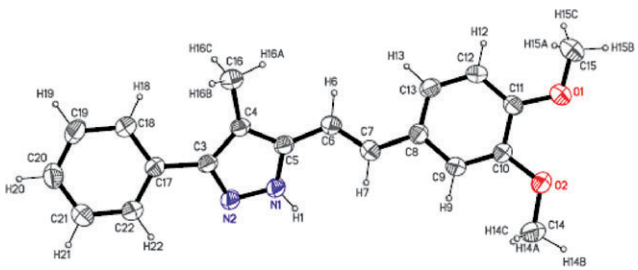

Fig. 7 The X-ray molecular structure of compound **8** (ORTEP plot, 35% probability for the ellipsoids).

NMR study

We have reported the ^{1}H, ^{13}C and ^{15}N NMR results concerning compounds **3**–**8** in Table 3, Table 4 and Table 5, respectively.

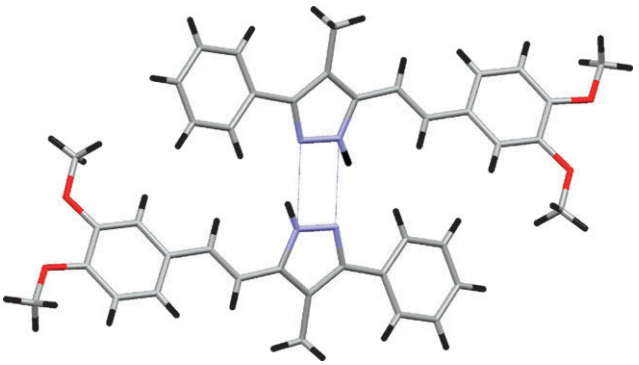

Fig. 8 The view along the a axis of **8**, showing the formation of dimers.

These data have been collected with the aim of determining the tautomeric equilibrium constants by simple integration. Although it has been pointed out that only ^{1}H NMR signal intensities are reliable for the determination of populations, in our experience, ^{13}C and ^{15}N signals can also been used in connection with signals related by tautomerism, *i.e.* carbon or nitrogen atoms linked to the same substituents.[3c] The assignments of the signals were based on standard 2D experiments, on the values of coupling constants (auto-consistency) and by comparison with other NH-pyrazoles where tautomerization is blocked.[21]

We have illustrated with one example the kind of spectra that we obtained (Fig. 9). The spectrum corresponds to compound **5** in HMPA-d_{18}, concentration 0.10 M and temperature 268 K (Table 4). The region of the methyl groups shows two narrow signals corresponding to the most abundant tautomer, and two broad signals corresponding to the less abundant one, as expected by simple consideration of the energy profile.

For compounds whose structure had not been determined by crystallography, we relied on CPMAS NMR results: **6b** and **7b** were the only tautomers present in the solid state (see Table 4 and Table 5). We are aware that solid state NMR and single crystal X-ray diffraction do not show exactly the same properties, for instance, static *vs.* dynamic disorder.[3b] To avoid further complications, we used fine powders for

 This journal is © The Royal Society of Chemistry and the Centre National de la Recherche Scientifique 2009

Downloaded on 02 January 2013
Published on 02 December 2008 on http://pubs.rsc.org | doi:10.1039/B812018H

Table 3 The ^{1}H NMR chemical shifts (δ) and ^{1}H–^{1}H coupling constants of compounds **3**–**8** (J/Hz) in DMSO-d_6 and HMPA-d_{18} solutions[a]

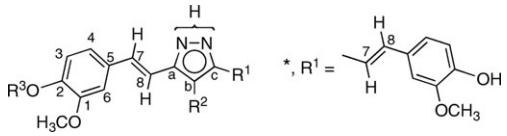

Compound	R^1	R^2	R^3	Solvent	Conc./M	T/K	NH	R^2	H3	H4	H6	OMe	OR^3	H7	H8	R^1	Tautomerism
3	*	H	H	DMSO	0.12	300	12.80	6.61 (H)	6.76	6.93	7.13	3.82	9.17 (H)	7.03	6.91	—	Average
4	CH_3	H	H	DMSO	0.07	300	12.40	6.20 (H)	6.74	6.91	7.12	3.81	9.15 (H)	6.95	6.88	2.19 (Me)	Average
				HMPA	0.07	300	13.26	6.11 (H)		6.85/7.16		3.80	10.26 (H)	6.85/7.16		2.23 (Me)	~50% **a**
				HMPA	0.07	300	13.20	6.11 (H)		6.85/7.16		3.80	10.24 (H)	6.85/7.16		2.15 (Me)	~50% **b**
				HMPA	0.10	276	13.34	6.19 (H)	6.85	6.85	7.06	3.80	10.42 (H)	7.20	6.87	2.25 (Me)	~50% **a**
				HMPA	0.10	276	13.27	6.11 (H)	6.85	6.85	7.06	3.80	10.34 (H)	6.92	6.83	2.14 (Me)	~50% **b**
5	CH_3	CH_3	H	DMSO	0.07	300	12.29	2.03 (Me)	6.75	6.91	7.13	3.83	9.08 (H)	6.95	6.86	2.10 (Me)	Average
				HMPA	0.10	300	13.16	2.04 (Me)	6.87	6.92	6.97	3.80	10.28 (H)	7.21	6.82	2.04 (Me)	35% **a**
				HMPA	0.10	300	13.10	2.04 (Me)	6.87	6.92	6.97	3.80	10.20 (H)	7.21	6.82	2.07 (Me)	65% **b**
				HMPA	0.10	268	13.25	2.05 (Me)	6.87	6.96	7.00	3.81	10.44 (H)	7.25	6.88	2.05 (Me)	35% **a**
				HMPA	0.10	268	13.20	2.05 (Me)	6.87	6.96	7.00	3.81	10.38 (H)	7.25	6.88	2.07 (Me)	65% **b**
6	C_6H_5	H	H	DMSO	0.11	300	12.96	6.88 (H)	6.78	6.96	7.15	3.84	9.10 (H)	7.10	6.95	7.80 (*o*) 7.43 (*m*) 7.31 (*p*)	36% **a**
				DMSO	0.11	300	13.18	6.88 (H)	6.78	6.96	7.15	3.84	9.21 (H)	7.10	6.95	7.80 (*o*) 7.43 (*m*) 7.31 (*p*)	64% **b**
7	C_6H_5	H	CH_3	DMSO	0.06	300	13.00	6.87 (H)	6.96	7.06	7.19	3.83	3.78 (Me)	7.14	7.03	7.80 (*o*) 7.43 (*m*) 7.32 (*p*)	40% **a**
				DMSO	0.06	300	13.21	6.87 (H)	6.96	7.06	7.19	3.83	3.78 (Me)	7.14	7.03	7.80 (*o*) 7.43 (*m*) 7.32 (*p*)	60% **b**
8	C_6H_5	CH_3	CH_3	DMSO	0.05	300	12.94	2.29 (Me)	6.95	7.07	7.25	3.84	3.77 (Me)	7.14	7.06	7.65 (*o*) 7.45 (*m*) 7.34 (*p*)	Rich in **b**
				HMPA	0.06	268	13.94	2.34 (Me)	7.09	7.09	7.25	3.88	3.84 (Me)	7.45	7.13	7.70 (*o*) 7.45 (*m*) 7.31 (*p*)	**b**

[a] The coupling constants were, on average: $^3J_{H3-H4}$ = 8.0 Hz, $^4J_{H4-H6}$ = 2.0 Hz (not always observed) and $^3J_{H7-H8_{trans}}$ = 16.5 Hz.

View Article Online

Table 4 The ^{13}C NMR chemical shifts (δ) and ^{1}H–^{13}C coupling constants (J/Hz) in DMSO-d_6 and HMPA-d_{18} solutions, and under CPMAS conditions[a]

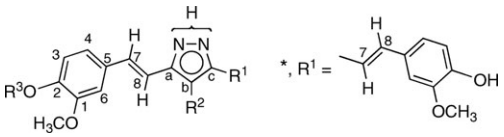

Compound	R^1	R^2	R^3	Solvent	Conc./M	T/K	Ca C4	Cb C5	Cc C6	R^2 C7	C1 C8	C2 OCH_3	C3 R^1	Tautomerism
3	*	H	H	DMSO	0.12	300	151.0 120.1	99.3 128.4	142.0 109.5	— (H) 129.8	147.9 112.9 (C8) 118.4 (C8′)	146.8 55.6	115.6	No tautomerism
				CPMAS	—	300	150.2 N.o.[b]	95.5 127.1	142.8 106.3	— (H) 129.9	147.4 111.9	145.1 53.5 56.5	114.5	No tautomerism
4	CH_3	H	H	DMSO	0.36	300	149.6 119.9	101.3 128.6	140.5 109.5	— (H) 129.0	147.9 117.4	146.6 55.6	115.7 11.6 (Me)	Average
				HMPA	0.10	276	150.9 119.4	100.0 128.4	142.4 110.5	— (H) 128.7	148.7 113.2	148.6 55.9	115.7 10.8 (Me-5)	~50% **a**
							138.4 119.6	101.6 128.4	148.9 110.5	— (H) 129.4	148.7 119.3	146.9 55.9	115.7 13.9 (Me-3)	~50% **b**
				CPMAS	—	300	151.5 120.5	101.1 129.9	142.4 113.2 115.3	— (H) 129.9	148.8 113.2	143.3 55.9	115.3 9.9 (Me-5)	**a**
5	CH_3	CH_3	H	DMSO	0.07	300	141.6 119.8	110.4 128.8	141.6 109.6	8.1 (Me) 127.9	147.9 114.9	146.6 55.7	115.6 10.6	Average
				HMPA	0.08	300	147.5 119.6	109.9 129.0	135.7 111.5	8.4 (Me) 127.7	149.0 118.7	148.7 56.3	116.1 11.9 (br)	35% **a**
				HMPA	0.08	300	138.3 119.6	109.9 129.0	145.8 111.5	8.4 (Me) 128.4	149.0 112.7	148.7 56.3	116.1 11.9 (br)	65% **b**
				HMPA	0.10	268	147.5 119.5	110.0 128.8	135.7 110.7	8.8 (br, Me) 127.6	148.8 118.5	148.6 55.9	115.8 9.1 (br)	35% **a**
				HMPA	0.10	268	138.3 119.5	109.9 128.8	145.8 110.7	8.4 (Me) 128.3	148.8 112.4	148.6 55.9	115.8 12.1	65% **b**
				CPMAS	—	300	145.9 123.4	110.2 130.9	138.6 105.5	9.8 (Me) 128.9	148.8 117.0	146.6 55.3	121.8 11.2 (br)	66% **a**
							137.5 123.4	112.0 130.9	146.6 105.5	9.8 (Me) 128.9	148.8 119.0	146.6 55.3	121.8 11.2 (br)	34% **b**
6	C_6H_5	H	H	DMSO	0.11	300	151.4 122.1	100.4 128.1	140.3 109.5	— (H) 130.1	147.9 118.4	146.6 55.5	115.3 132.0 (*i*) 125.0 (*o*) 128.7 (*m*) 127.5 (*p*)	36% **a**
				DMSO	0.11	300	142.6 120.2	99.5 128.1	151.0 109.5	— (H) 130.1	147.9 112.7	147.1 55.6	115.6 133.6 (*i*) 125.1 (*o*) 128.7 (*m*) 127.5 (*p*)	64% **b**
6b	C_6H_5	H	H	CPMAS	—	300	144.0 116.0	103.5 129.0	152.6 112.3	— (H) 129.0	148.3 113.5	116.0 54.0	133.2 (*i*) 126.4 (*o*) 129.0 (*m*) 129.0 (*p*)	
7	C_6H_5	H	CH_3	DMSO	0.11	300	151.3 119.4	99.2 129.4	142.8 108.9	— (H) 128.9	149.0 113.6	149.0 55.51 (C1) 55.45 (C2)	111.9 133.7 (*i*) 125.0 (*o*) 128.6 (*m*) 127.4 (*p*)	40% **a**
				DMSO	0.11	300	142.4 119.9	99.8 129.4	150.9 108.9	— (H) 129.7	149.0 113.6	149.0 55.51 (C1) 55.45 (C2)	111.9 133.7 (*i*) 125.0 (*o*) 128.6 (*m*) 127.4 (*p*)	60% **b**

Published on 02 December 2008 on http://pubs.rsc.org | doi:10.1039/B812018H
Downloaded on 02 January 2013

 This journal is © The Royal Society of Chemistry and the Centre National de la Recherche Scientifique 2009

Table 4 (*continued*)

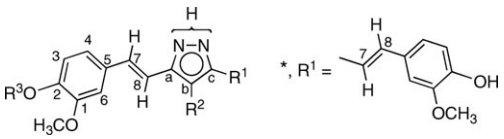

Compound	R^1	R^2	R^3	Solvent	Conc./M	T/K	Ca C4	Cb C5	Cc C6	R^2 C7	C1 C8	C2 OCH_3	C3 R^1	Tautomerism
7b	C_6H_5	H	CH_3	CPMAS	—	300	143.1 120.9	96.3 129.1	149.8 108.0	— (H) 129.1	148.8 110.6	148.8 53.5 (C1*) 56.1 (C2*)	110.6 132.1 (*i*) 125.2 (*o*) 129.1 (*m*) 126.2 (*p*)	
8	C_6H_5	CH_3	CH_3	DMSO	0.31	300	141.7 119.9	110.7 130.0	147.1 109.1	9.4 (Me) 128.4	149.1 114.5	148.8 55.6 (C1) 55.5 (C2)	111.9 133.2 (*i*) 127.1 (*o*) 128.5 (*m*) 127.3 (*p*)	Aver. Rich in **b**
				HMPA	0.06	268	139.7 120.2	110.4 130.9	149.5 109.1	10.1 (Me) 128.8	149.8 113.2	149.3 55.9 (C1) 55.9 (C2)	112.1 135.9 (*i*) 127.2 (*o*) 128.6 (*m*) 126.9 (*p*)	**b**
				CPMAS	—	300	140.7 124.7	112.5 130.2	148.8 110.7	9.2 (Me) 130.2	148.8 117.1	148.8 54.7	112.5 134.6 (*i*) 128.5 (*o*) 130.2 (*m*) 126.7 (*p*)	**b**

[a] The ^1J coupling constants are not reported; their average values are: pyrazole C4–Hb = 175 Hz; phenyl CH = 159 Hz except C4–H and C6–H = 156 Hz; olefin C–H = 155 Hz; OCH_3 = 144 Hz; C–Me substituents: 126.5 Hz. The other couplings (Hz) are: ^2J = 2.2 (C1), ^2J = 4.5 (C7), ^2J = 5.9 (Cb–Me4); ^3J = 8.4 (C1), ^3J = 7.3 (C2), ^3J = 5.8 (C4), ^3J = 6.8 (C5), ^3J = 6.0 (C6), ^3J = 4.5 (C7), ^3J = 2.4 (Cb–H). [b] Not observed.

Published on 02 December 2008 on http://pubs.rsc.org | doi:10.1039/B812018H
Downloaded on 02 January 2013

CPMAS NMR, obtained by grinding the same batch of crystals that we used for X-ray crystallography.

Percentages of tautomers and equilibrium constants

Although some exceptions are known, the assumption of the identical nature of the most stable tautomer in solution and the tautomer present in the crystal is one of the most basic tenets in tautomerism.[3b,3c,17b] The results in Table 6 confirm this principle for compounds **4**, **5** and **8**, and allow us to conclude that in the solid state, **6** should crystallize as **6b** and **7** as **7b**, or at least in cyclamers where **6b** and **7b** are predominant.

Compound **5** exists in the solid state as a 66% **5a**/34% **5b** mixture and in HMPA as a 35% **5a**/65% **5b** mixture, thus being an exception to the rule of similarity between solution and solid state. However, the difference in energy at 300 K between the two situations is only of 3.2 kJ mol^{-1}.

Conclusions

The structure, tautomerism and absence of SSPT have been determined for six NH-pyrazoles by a combination of X-ray crystallography and $^{13}C/^{15}N$ NMR spectroscopy. Two of the conditions required to observe SSPT in NH-pyrazoles are the identity (or, at least, strong similarity) of the substituents at the 3- and 5-positions, and the formation of cyclic structures, cyclamers, linked by N–H···N hydrogen bonds. Compound **3** has the same substituent at both positions (tautomer **3a** is identical to tautomer **3b**), but crystallizes in a complex network of hydrogen bonds involving the OH groups. Compound **8** crystallizes as a dimer, but with only one tautomer present (**8a**). Thus, none of the compounds of Table 6 display SSPT. Finally, compound **5** is the only known example of an NH-pyrazole that crystallizes as a 2 : 1 mixture of two tautomers (there are examples of 2 : 2 and 3 : 1 mixtures, but in cyclic tetramers[17b,22]).

Experimental

The melting points of pyrazoles **3**–**8** were determined by differential scanning calorimetry (DSC) on a Seiko DSC 220C connected to a Model SSC5200H Disk Station; for the other compounds, a hot stage microscope was used. Thermograms (sample size 0.003–0.0010 g) were recorded at a scanning rate of 2.0 °C min^{-1}. Thin-layer chromatography (TLC) was performed using Merck silica gel (60 F_{254}) and compounds were detected with a 254 nm UV lamp. Silica gel (60–320 mesh) was employed for routine column chromatography separations. Elemental analyses for carbon, hydrogen and nitrogen were carried out by the Microanalytical Service of the Universidad Complutense of Madrid on a Perkin-Elmer 240 analyzer.

Downloaded on 02 January 2013
Published on 02 December 2008 on http://pubs.rsc.org | doi:10.1039/B812018H

Table 5 The ^{15}N NMR chemical shifts (δ) in DMSO-d_6 and HMPA-d_{18} solutions, and under CPMAS conditions

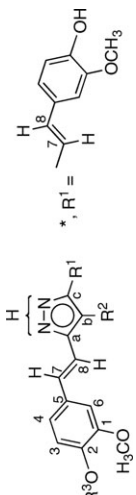

Compound	R^1	R^2	R^3	Solvent	Conc./M	T/K	N–H	–N=	% a	% b	PT[a]
3	*	H	H	CPMAS	—	300	−180.8	−100.6	50	50	No
4	CH_3	H	H	HMPA	0.10	276	−180.5	N.o.[b]	~50	~50	No
							−173.6				
4a	CH_3	H	H	CPMAS	—	300	−177.7	−100.9	100	0	No
5	CH_3	CH_3	H	HMPA	0.08	300	−185.6 (major)	N.o.	30	70	No
							−175.9				
				CPMAS	—	300	−187.8	−111.2	66	34	No
							−172.0 (major)	−103.6 (major)			
6b	C_6H_5	H	H	CPMAS	—	300	−181.5	−105.3	0	100	No
8b	C_6H_5	CH_3	CH_3	HMPA	0.06	268	−182.2	N.o.	0	100	No
				CPMAS	—	300	−181.3	−98.7	0	100	No

[a] Proton transfer [b] Not observed

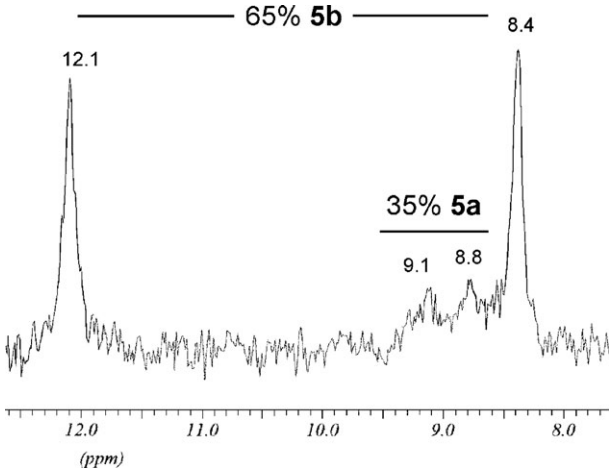

Fig. 9 The methyl group region of the ^{13}C NMR spectrum of **5**.

General procedure for the preparation of pyrazole derivatives (3–8)

Compounds **3**–**8** were prepared by reacting the corresponding β-diketones[23] (1 mmol) with hydrazine hydrate 98% (1.5 mmol) in acetic acid (5 mL). After heating at reflux for 2 h, the reaction mixture was poured into water, and the precipitate filtered off, washed with water and dried. The solid was purified by column chromatography using ethyl acetate as the eluent.

(*E*)-3,5-Bis[β-(4-hydroxy-3-methoxyphenyl)-ethenyl]-1*H*-pyrazole (3)

3 was prepared from purified commercially available **1**. The compound was obtained as a colourless solid after recrystallization from H_2O/EtOH (1 g, 2.74 mmol, 63%). Mp: 217.1 °C, lit.: 211–214 °C[5] or 215 °C.[8] Anal. calc. for $C_{21}H_{20}N_2O_4$ (364.14): C, 69.22; H, 5.53; N, 7.69; found: C, 68.79; H, 5.53; N, 7.70%.

(*E*)-3(5)-[β-(4-hydroxy-3-methoxyphenyl)-ethenyl]-5(3)-methyl-1*H*-pyrazole (4)

4 was prepared from (*E*)-6-(4-hydroxy-3-methoxyphenyl)hex-5-ene-2,4-dione.[23] The compound was obtained as a colourless solid after recrystallization from CH_2Cl_2/hexane/EtOH (251 mg, 1.1 mmol, 85%). Mp: 141.6 °C. Anal. calc. for $C_{13}H_{14}N_2O_2$ (230.11): C, 67.26; H, 6.44; N, 12.11; found: C, 67.81; H, 6.13; N, 12.17%.

(*E*)-3(5)-[β-(4-hydroxy-3-methoxyphenyl)-ethenyl]-4,5(3)-dimethyl-1*H*-pyrazole (5)

5 was prepared from (*E*)-6-(4-hydroxy-3-methoxyphenyl)-3-methylhex-5-ene-2,4-dione.[23] The compound was obtained as a colourless solid after recrystallization from CH_2Cl_2/hexane/EtOH (180 mg, 0.73 mmol, 61%). Mp: 176.1 °C. Anal. calc. for $C_{14}H_{16}N_2O_2$ (244.12): C, 68.46; H, 6.61; N, 11.35; found: C, 68.83; H, 6.60; N, 11.47%.

 This journal is © The Royal Society of Chemistry and the Centre National de la Recherche Scientifique 2009

Published on 02 December 2008 on http://pubs.rsc.org | doi:10.1039/B812018H
Downloaded on 02 January 2013

Table 6 The tautomeric composition of **3**–**8** (Sty: Ar–CH═CH–)[a]

Compound	Tautomers	X-Ray	CPMAS	DMSO	HMPA
3	**a**, **b**: 3,5-BisSty	**3a** = **3b**	**3a** = **3b**	**3a** = **3b** No PT[b]	N. M.
4	**a**: 3-Sty-5-Me	**4a**	**4a**	Average rich in **4a**	~50% **4a**
	b: 3-Me-5-Sty				~50% **4b**
5	**a**: 3-Sty-5-Me	66% **5a**	66% **5a**	Average rich in **5b**	35% **5a**
	b: 3-Me-5-Sty	34% **5b**	34% **5b**		65% **5b**
6	**a**: 3-Sty-5-Ph	N. M.	**6b**	36% **6a**	N. M.
	b: 3-Ph-5-Sty			64% **6b**	
7	**a**: 3-Sty-5-Ph	N. M.	**7b**	40% **7a**	N. M.
	b: 3-Ph-5-Sty			60% **7b**	
8	**a**: 3-Sty-5-Ph	**8b**	**8b**	Average rich in **8b**	**8b**
	b: 3-Ph-5-Sty				

[a] N. M. means not measured. [b] Proton transfer

Table 7 The crystal and structure refinement data for compounds **3**, **4**, **5** and **8**

Crystal data		**3**	**4**	**5**	**8**
Empirical formula		$C_{21}H_{20}N_2O_4$	$C_{13}H_{14}N_2O_2$	$C_{14}H_{16}N_2O_2$	$C_{20}H_{20}N_2O_2$
Formula weight		364.39	230.26	244.29	320.38
Crystal system		Monoclinic	Orthorhombic	Monoclinic	Orthorhombic
Space group		*P*2(1)/*c*	*Pbca*	*P*2(1)/*c*	*Pbca*
Unit cell dimensions	*a*/Å	8.2394(10)	13.2563(15)	8.519(2)	13.2363(13)
	b/Å	14.0198(17)	7.6962(9)	12.964(4)	8.2769(8)
	c/Å	16.306(2)	22.855(3)	34.615(10)	30.673(3)
	β (°)	101.060(3)	—	94.607(7)	—
Volume/Å^3		1848.7(4)	2331.7(5)	3810.6(19)	3360.4(6)
Z		4	8	12	8
Density (calculated)/Mg m^{-3}		1.309	1.312	1.277	1.267
Absorption coefficient/mm^{-1}		0.092	0.090	0.087	0.083
Scan technique		ω and φ	ω and φ	ω and φ	ω and φ
F(000)		768	976	1560	1360
Range for data collection (°)		1.93 to 25.00	1.78 to 27.00	1.18 to 25.00	1.33 to 25.00
Index ranges		−9, −16, −18 to 9, 16, 19	−13, −9, −29 to 16, 9, 29	−9, −15, −41 to 10, 15, 41	−15, −9, −36 to 10, 9, 32
Reflections collected		13 998	19 397	28 784	16 484
Independent reflections		3244	2541	6720	2954
Observed reflections [$I > 2\sigma(I)$]		1418	1248	2855	1655
R_{int}		0.1198	0.0889	0.0905	0.0708
Completeness to θ (%)		99.6	100.0	100.0	99.9
Data/restraints/parameters		3244/0/245	2541/0/156	6720/2/497	2954/0/224
Goodness-of-fit on F^2		0.912	1.034	0.984	1.074
$R1^a$		0.0539	0.0508	0.0769	0.0507
w$R2^b$ (all data)		0.1808	0.1768	0.2486	0.1848
Largest differential peak and hole/eÅ^{-3}		0.232 and −0.278	0.214 and −0.247	0.950 and −0.377	0.193 and −0.192

[a] $R1 = \sum||F_o| - |F_c||/\sum|F_o|$. [b] $wR2 = \sum[w(F_o^2 - F_c^2)^2]/\sum[w(F_o^2)]$.

(*E*)-3(5)-[β-(4-hydroxy-3-methoxyphenyl)-ethenyl]-5(3)-phenyl-1*H*-pyrazole (6)

6 was prepared from (*E*)-5-(4-hydroxy-3-methoxyphenyl)-1-phenylpent-4-ene-1,3-dione.[23] The compound was obtained as a colourless solid after recrystallization from CH_2Cl_2/hexane/EtOH (228 mg, 0.78 mmol, 77%). Mp: 142.9 °C. Anal. calc. for $C_{18}H_{16}N_2O_2$ (292.12): C, 73.95; H, 5.54; N, 10.11; found: C, 73.95; H, 5.54; N, 10.11%.

(*E*)-3(5)-[β-(3,4-dimethoxyphenyl)-ethenyl]-5(3)-phenyl-1*H*-pyrazole (7)

7 was prepared from (*E*)-5-(3,4-dimethoxyphenyl)-1-phenylpent-4-ene-1,3-dione.[23] The compound was obtained as a colourless solid after recrystallization from CH_2Cl_2/hexane/EtOH (196 mg, 1.27 mmol, 51%). Mp: 173.4 °C. Anal. calc. for $C_{19}H_{18}N_2O_2$ (306.37): C, 74.48; H, 5.92; N, 9.14; found: C, 74.21; H, 5.82; N, 9.16%.

(*E*)-3(5)-[β-(3,4-dimethoxyphenyl)-ethenyl]-4-methyl-5(3)-phenyl-1*H*-pyrazole (8)

8 was prepared from (*E*)-5-(3,4-dimethoxyphenyl)-2-methyl-1-phenylpent-4-ene-1,3-dione.[23] The compound was obtained as a colourless solid after recrystallization from CH_2Cl_2/hexane/EtOH (170 mg, 0.53 mmol, 58%). Mp: 182.0 °C. Anal. calc. for $C_{20}H_{20}N_2O_2$ (320.39): C, 74.97; H, 6.29; N, 8.74; found: C, 74.28; H, 6.14; N, 8.77%.

X-Ray data collection and structure refinement (compounds 3, 4, 5 and 8)

Data collection for all of the compounds was carried out at room temperature on a Bruker Smart CCD diffractometer

Published on 02 December 2008 on http://pubs.rsc.org | doi:10.1039/B812018H
Downloaded on 02 January 2013

using graphite-monochromated Mo-Kα radiation (λ = 0.71073 Å) operating at 50 kV and 30 mA. In all cases, the data were collected over a hemisphere of the reciprocal space by the combination of three exposure sets. Each frame exposure time was either 10 or 20 s, covering 0.3° in ω. The cell parameters were determined and refined by a least-squares fit of all reflections collected. The first 100 frames were recollected at the end of the data collection to monitor crystal decay, and no appreciable decay was observed. A summary of the fundamental crystal and refinement data is given in Table 7. The structures of all the compounds were solved by direct methods and conventional Fourier synthesis, and refined by full matrix least-squares on F^2 (SHELXL-97).[24] All non-hydrogen atoms were refined anisotropically.

In all cases, the hydrogen atoms were calculated, included and refined as riding on their respective carbon-bonded atom with a common anisotropic displacement. The rest of the hydrogen atoms, *i.e.* those bonded to nitrogen or oxygen atoms, were located in a Fourier difference synthesis, and in all cases were included and refined as riding on their respective bonded atoms for **3**, **4** and **5**, while for **8**, its coordinates were refined and the thermal factors kept constant. The longer O–H bond distances in some of the hydroxyl groups are due to the formation of hydrogen bonds.[25]

The largest peaks and holes in the final difference map were 0.232 and −0.278, 0.214 and −0.247, 0.950 and −0.377, and 0.193 and −0.192 eÅ^{-3} for **3**, **4**, **5** and **8**, respectively. The final $R1$ and w$R2$ values were 0.0539 and 0.1808, 0.0508 and 0.1768, 0.0769 and 0.2486, and 0.0507 and 0.1848 for **3**, **4**, **5** and **8**, respectively.

NMR spectroscopy

Solution NMR spectra. Solution NMR spectra were recorded on a Bruker DRX 400 (9.4 T; 400.13 MHz for ^{1}H, 100.62 MHz for ^{13}C and 40.56 MHz for ^{15}N) spectrometer fitted with a 5 mm inverse detection H–X probe and equipped with a z-gradient coil at 300 K. ^{1}H and ^{13}C NMR chemical shifts (δ) are referenced to Me_4Si; for ^{15}N NMR, nitromethane (0.00) was used as an external standard. Typical parameters for the ^{1}H NMR spectra were: a spectral width of 5787 Hz, a pulse width of 7.5 µs, an attenuation level of 0 dB and a resolution of 0.34 Hz per point. Typical parameters for the ^{13}C NMR spectra were: a spectral width of 21 kHz, a pulse width of 10.6 µs, an attenuation level of −6 dB, a relaxation delay of 2 s and a resolution of 0.63 Hz per point; WALTZ-16 was used for broadband proton decoupling and the FIDs were multiplied by an exponential weighting (lb = 1 Hz) before Fourier transformation. 2D inverse proton detected heteronuclear shift correlation spectra, gs-HMQC (^{1}H–^{13}C) and gs-HMBC (^{1}H–^{13}C), were acquired and processed using standard Bruker NMR software. Typical parameters for these spectra were: a spectral width of 5787 Hz for ^{1}H and 20.5 kHz for ^{13}C, a 1024 × 256 data set, number of scans = 2 (gs-HMQC) or 4 (gs-HMBC), a relaxation delay of 1 s, and a delay for the evolution of ^{13}C–^{1}H coupling constants of 3 ms (gs-HMQC) or 60 ms (gs-HMBC). The FIDs were processed using zero filling in the $F1$ domain, and a sine-bell window function in both dimensions was applied prior to Fourier transformation. In the gs-HMQC experiments, GARP modulation of ^{13}C was used for decoupling. ^{15}N NMR spectra were acquired using 2D inverse proton detected heteronuclear shift correlation spectroscopy. Typical parameters for the gs-HMQC (^{1}H–^{15}N) spectra were: a spectral width of 5787 Hz for ^{1}H and 12.5 kHz for ^{15}N, a 1024 × 256 data set, number of scans = 4, a relaxation delay of 1 s and a 7 ms delay for the evolution of the ^{15}N–^{1}H coupling. The FIDs were processed using zero filling in the $F1$ domain, and a sine-bell window function in both dimensions was applied prior to Fourier transformation. A Bruker BVT 3000 temperature unit was used to control the temperature of the cooling gas stream and an exchanger was used to achieve low temperatures.

Solid state. Solid state ^{13}C (100.73 MHz) and ^{15}N (40.60 MHz) CPMAS NMR spectra were recorded on a Bruker WB 400 spectrometer at 300 K using a 4 mm DVT probe head. Samples were carefully packed in 4 mm diameter cylindrical zirconia rotors with Kel-F caps. Operating conditions involved 90 3.2 µs ^{1}H pulses and a decoupling field strength of 78.1 kHz in a TPPM sequence. The non-quaternary suppression (NQS) technique to observe only the quaternary carbon atoms was employed. ^{13}C spectra were initially referenced to a glycine sample and then the chemical shifts were recalculated to Me_4Si (for the carbonyl atom, $\delta_{glycine}$ = 176.1). Similarly, ^{15}N spectra were initially referenced to $^{15}NH_4Cl$ and then recalculated to nitromethane, using the relationship: $\delta\ ^{15}N_{nitromethane} = \delta\ ^{15}N_{NH_4Cl} - 338.1$. Typical acquisition parameters for the ^{13}C CPMAS were: a spectral width of 40 kHz, a recycle delay of 15–75 s, an acquisition time of 30 ms, a contact time of 2 ms and a spin rate of 12 kHz. Typical parameters for the ^{15}N CPMAS were: a spectral width of 40 kHz, a recycle delay of 15–75 s, an acquisition time of 35 ms, a contact time of 7–8 ms and spin rate of 6 kHz.

Acknowledgements

This work has been financed by the Spanish MEC (CTQ2006-02586 and CTQ2007-62113).

References

1 J. Higdon, *Curcumin*, Linus Pauling Institute, Oregon State University, Oregon, USA (http://lpi.oregonstate.edu/infocenter/phytochemicals/curcumin/).
2 (*a*) R. M. Claramunt, D. Sanz del Castillo, J. Elguero, P. Nioche, C. S. Raman, P. Martasek and B. S. S. Masters, XVIIth International Symposium on Medicinal Chemistry, Poster P101, *Drugs Future*, 2002, **27**(Suppl. A), 177; (*b*) C. Pérez-Medina, M. Pérez-Torralba, C. López, R. M. Claramunt, P. Nioche and C. S. Raman, *XIV Congreso Nacional de la Sociedad Española de Química Terapeútica*, Bilbao, Spain, 2005.
3 (*a*) J. Elguero, C. Marzin, A. R. Katritzky and P. Linda, *The Tautomerism of Heterocycles*, Academic Press, New York, 1976, pp. 655; (*b*) V. I. Minkin, A. D. Garnosvskii, J. Elguero, A. R. Katritzky and O. V. Denisko, *Adv. Heterocycl. Chem.*, 2000, **76**, 157–323; (*c*) R. M. Claramunt, C. López, M. D. Santa María, D. Sanz and J. Elguero, *Prog. Nucl. Magn. Reson. Spectrosc.*, 2006, **49**, 169–206.
4 (*a*) J. Quiroga Puello, B. Insuasty Obando, C. Foces-Foces, L. Infantes, R. M. Claramunt, P. Cabildo, J. A. Jimenez and J. Elguero, *Tetrahedron*, 1997, **53**, 10783–10802; (*b*) M. H. Holschbach, D. Sanz, R. M. Claramunt, L. Infantes, S. Motherwell, P. R. Raithby, M. L. Jimeno, D. Herrero,

 This journal is © The Royal Society of Chemistry and the Centre National de la Recherche Scientifique 2009

View Article Online

Published on 02 December 2008 on http://pubs.rsc.org | doi:10.1039/B812018H
Downloaded on 02 January 2013

I. Alkorta, N. Jagerovic and J. Elguero, *J. Org. Chem.*, 2003, **68**, 8831–8837; (*c*) R. M. Claramunt, M. Á. García, C. López, S. Trofimenko, G. P. A. Yap, I. Alkorta and J. Elguero, *Magn. Reson. Chem.*, 2005, **43**, 89–91; (*d*) S. Trofimenko, G. P. A. Yap, F. A. Jove, R. M. Claramunt, M. Á. García, M. D. Santa María, I. Alkorta and J. Elguero, *Tetrahedron*, 2007, **63**, 8104–8111.

5 D. L. Flynn, T. R. Belliotti, A. M. Boctor, D. Connor, C. Kostlan, D. E. Nies, D. F. Ortwine, D. J. Schrier and J. C. Sircar, *J. Med. Chem.*, 1991, **34**, 518–525.

6 J. S. Shim, D. H. Kim, H. J. Jung, J. H. Kim, D. Lim, S.-K. Lee, K.-W. Kim, J. W. Ahn, J.-S. Yoo, J.-R. Rho, J. Shin and H. J. Kwon, *Bioorg. Med. Chem.*, 2002, **10**, 2439–2444.

7 J. Ishida, H. Ohtsu, Y. Tachibana, Y. Nakanishi, K. F. Bastow, M. Nagai, H.-K. Wang, H. Itokawa and K.-H. Lee, *Bioorg. Med. Chem.*, 2002, **10**, 3481–3487.

8 H. Ohtsu, Z. Xiao, J. Ishida, M. Nagai, H.-K. Wang, H. Itogawa, C.-Y. Su, C. Shih, T. Chiang, E. Chang, Y. Lee, M.-Y. Tsai, C. Chang and K.-H. Lee, *J. Med. Chem.*, 2002, **45**, 5037–5042.

9 C. Selvam, S. M. Jachak, R. Thilagavathi and A. K. Chakraborti, *Bioorg. Med. Chem.Lett.*, 2005, **15**, 1793–1797.

10 R. Narlawar, K. Baumann, R. Schubenel and B. Schmidt, *Neurodegener. Dis.*, 2007, **4**, 88–93.

11 R. Narlawar, M. Pickhardt, S. Leuchtenberger, K. Baumann, S. Krause, T. Dyrks, S. Weggen, E. Mandelkow and B. Schmidt, *ChemMedChem*, 2008, **3**, 165–172.

12 P. Maher, T. Akaishi, D. Schubert and K. Abe, *Neurobiol. Aging*, 2008, DOI: 10.1016/j.neurobiolaging.2008.05.020.

13 (*a*) J. Elguero, in *Comprehensive Heterocyclic Chemistry*, ed. A. R. Katritzky and C. W. Rees, Pergamon Press, Oxford, 1984, vol. **5**, pp. 167; (*b*) J. Elguero, in *Comprehensive Heterocyclic Chemistry II*, ed. A. R. Katritzky, C. W. Rees and E. F. Scriven, Pergamon Press, Oxford, 1996, vol. **3**, pp. 1; (*c*) B. Stanovnik and J. Svete, in *Science of Synthesis*, ed. R. Neier, Thieme, Stuttgart, 2002, vol. **12**, ch. 12.1.

14 B. B. Aggarwal, A. Kumar, M. S. Aggarwal and S. Shishodia, Curcumin Derived from Tumeric (*Curcuma longa*): a Spice for All Seasons, in *Phytopharmaceuticals in Cancer Chemoprevention*, ed. D. Bagchi and H. G. Preuss, CRC Press, Boca Raton, 2005, pp. 349–387.

15 I. Alkorta, J. Elguero, B. Donnadieu, M. Etienne, J. Jaffart, D. Schagen and H.-H. Limbach, *New J. Chem.*, 1999, **23**, 1231–1237.

16 (*a*) C. Foces-Foces, I. Alkorta and J. Elguero, *Acta Crystallogr., Sect. B: Struct. Sci.*, 2000, **56**, 1018–1028; (*b*) I. Alkorta, J. Elguero, C. Foces-Foces and L. Infantes, *ARKIVOC (Gainesville, FL, U. S.)*, 2006, **ii**, 15–30.

17 (*a*) R. M. Claramunt, P. Cornago, V. Torres, E. Pinilla, M. R. Torres, A. Samat, V. Lokshin, M. Valés and J. Elguero, *J. Org. Chem.*, 2006, **71**, 6881–6891; (*b*) R. M. Claramunt, P. Cornago, M. D. Santa María, V. Torres, E. Pinilla, M. R. Torres and J. Elguero, *Supramol. Chem.*, 2006, **18**, 349–356.

18 C. Foces-Foces, C. Cativiela, J. L. Serrano, M. M. Zurbano, N. Jagerovic and J. Elguero, *J. Chem. Crystallogr.*, 1996, **26**, 127–131.

19 (*a*) A. M. S. Silva, L. M. P. M. Almeida, J. A. S. Cavaleiro, C. Foces-Foces, A. L. Llamas-Saiz, C. Fontenas, N. Jagerovic and J. Elguero, *Tetrahedron*, 1997, **53**, 11645–11658; (*b*) D. C. G. A. Pinto, A. M. S. Silva, J. A. S. Cavaleiro, C. Foces-Foces, A. L. Llamas-Saiz, N. Jagerovic and J. Elguero, *Tetrahedron*, 1999, **55**, 10187–10200.

20 C. Foces-Foces, A. Echevarría, N. Jagerovic, I. Alkorta, J. Elguero, U. Langer, O. Klein, M. Minguet-Bonvehí and H.-H. Limbach, *J. Am. Chem. Soc.*, 2001, **123**, 7898–7906.

21 M. Begtrup, G. Boyer, P. Cabildo, C. Cativiela, R. M. Claramunt, J. Elguero, J. I. García, C. Toiron and P. Vedsø, *Magn. Reson. Chem.*, 1993, **31**, 107–168.

22 J. Elguero, N. Jagerovic, C. Foces-Foces, F. H. Cano, M. V. Roux, F. Aguilar-Parrilla and H.-H. Limbach, *J. Heterocycl. Chem.*, 1995, **32**, 451–456.

23 P. Cornago, R. M. Claramunt, L. Bouissane, I. Alkorta and J. Elguero, *Tetrahedron*, 2008, **64**, 8089–8094.

24 G. M. Sheldrick, *SHELXL-97, Program for refinement of crystal structures*, University of Göttingen, Germany, 1997.

25 G. R. Desiraju and T. Steiner, *The Weak Hydrogen Bond in Structural Chemistry and Biology*, Oxford University Press, Oxford, 1999.